Temporal scaling characteristics of diffusion as a new MRI contrast: Findings in rat hippocampus

Evren Ozarslan[1,2], Timothy M Shepherd[3], Cheng Guan Koay[4], Stephen J Blackband[5], and Peter J Basser[1]

[1]*STBB / PPITS / NICHD, National Institutes of Health, Bethesda, MD, United States,* [2]*Center for Neuroscience and Regenerative Medicine, USUHS, Bethesda, MD, United States,* [3]*University of California, San Francisco, CA,* [4]*University of Wisconsin, Madison, WI,* [5]*University of Florida, Gainesville, FL*

INTRODUCTION: Diffusion-weighted acquisitions with multiple diffusion-times can be analyzed within a theoretical framework developed for disordered media and fractals [1]. This approach can be justified for neural tissue due to its extremely complicated and hierarchical structure. In such environments, the diffusion propagator is expected to obey the temporal scaling (TS) relationships $\langle z^2\rangle \propto \Delta^{2/d_w}$ and $P_1(0) \propto \Delta^{-d_s'/2}$, where $\langle z^2\rangle$ is the mean squared displacement, Δ is the diffusion time, $P_1(0)$ is the probability for zero net displacement, d_w is the fractal dimension for the random walk, and d_s' is the spectral (fracton) dimension for the one dimensional propagator. The TS parameters d_w and d_s' deviate from their "normal" values of 2 and 1 when diffusion is anomalous. Further, these two dynamic parameters can be used to compute an apparent fractal dimension of the medium through the relationship $d_f' = d_w\, d_s'/2$. The slope of the q-space MR signal decay in the low-q regime enables the estimation of $\langle z^2\rangle$ (hence d_w), while the integral of the entire signal decay profiles is evaluated to estimate $P_1(0)$ (hence d_s'). In this study, we show experimental results obtained from excised rat hippocampi using a novel numerical procedure to mitigate any noise-induced bias, and discuss the contrast attained in TS parameter maps.

IMAGE ACQUISITION: Diffusion-weighted MR images were collected from four excised rat hippocampi at 14 T. The first sample (sample A) was imaged at 17 °C using a pulsed gradient stimulated-echo pulse sequence with the following parameters: TR=1 s, TE=12.6 ms, bandwidth=35 kHz, resolution=(78×78×500) μm^3, matrix=(64×64×4), δ=2 ms. Images were acquired with 32 diffusion gradient strengths (applied along the slice direction) increasing from 91.75 to 2935 mT/m. This q-space acquisition scheme was repeated for 5 diffusion pulse separations (Δ) ranging from 12 to 210 ms on a logarithmic scale. The same specimen underwent a series of four diffusion tensor imaging (DTI) scans. The diffusion times were 12.0, 24.5, 103, and 210 ms, respectively. Each data set consisted of a total of 27 scans—6 at low diffusion-weightings, 21 at the b-value of 1280 s/mm^2. To assess the reproducibility of the TS features at physiologically more relevant conditions, the remaining three specimens, (B1, B2, and B3) were imaged at 37 °C using a similar protocol with 8 diffusion time values ranging from 12 to 147 ms. To prevent the bias that can be introduced by processes that may occur during the experiment, such as autolysis, the ordering of experiments with different diffusion times was randomized.

PARAMETER ESTIMATION: Accurate estimation of the TS exponents proves to be a challenging task when there is significant noise in the data. Any bias introduced by noise is expected to shift the estimates of the TS parameters. To overcome this serious issue, we devised a procedure consisting of the following steps: (i) The standard deviation of the underlying Gaussian noise was estimated using the PIESNO framework [2]. (ii) The signal profile was represented in an orthogonal basis of Hermite functions [3]. (iii) Any bias due to the Rician character of the signal was eliminated [4] by transforming the data to Gaussian values. (iv) Step ii was repeated for the bias-corrected signal. (v) Using analytical relations, the moments of the propagator as well as the zero net displacement probability were computed using analytical relationships. (vi) A robust linear fitting was employed to compute the exponent characterizing the TS of the moments and zero displacement probability.

RESULTS & DISCUSSION: Figure 1 shows the TS parameter maps and traditional maps of apparent diffusion coefficient (ADC) and DTI-derived indices for sample A. Clearly, the TS parameter maps yield contrast that is not available in the traditional images. Diffusion in the granule cell and pyramidal cell layers is well within the subdiffusion regime (d_w>2). These regions are composed of densely packed neuronal cell bodies and proximal apical and basal dendrites that could lead to such behavior. The d_w values for all other hippocampal regions have limited variability (d_w≈2), suggesting normal diffusion.

Figure 2 shows the TS maps for the B1 and B2 specimens. The consistency of the TS parameter estimates demonstrates their reproducibility across specimens as well as the robustness of the estimation methods. The smaller maps illustrate the linear correlation coefficients, which indicate the adequacy of the hypothesized power-laws.

The DTI acquisitions with different diffusion times were used to assess the TS of diffusion anisotropy as well as the anisotropy of TS. As an example, the d_w estimates for three different gradient orientations are shown in Fig. 3A. Anisotropy in the d_w estimates is depicted in Fig. 3B. TS in most regions of the hippocampus appears to be weakly anisotropic though significant anisotropy is observed in certain regions with pyramidal neurons and white-matter regions of fimbria, alveus, and DHC.

CONCLUSION: We exploited the diffusion-time dependence of several q-space MR derived parameters to generate new forms of contrast in neural tissue, providing unique information about its cytoarchitecture. Such information could be sensitive to alterations due to numerous pathologies, development, and aging. TS contrast was observed to be reproducible in different specimens and under different conditions, which suggests the possibility of employing the method in population studies.

References: [1] Ozarslan et al., *J Magn Reson*, 183, p. 315, 2006. [2] Koay et al., *J Magn Reson*, 199, p. 94, 2009. [3] Ozarslan et al., *New J Phys*, 13, 015010, 2011. [4] Koay et al., *J Magn Reson*, 197, p. 108, 2009.

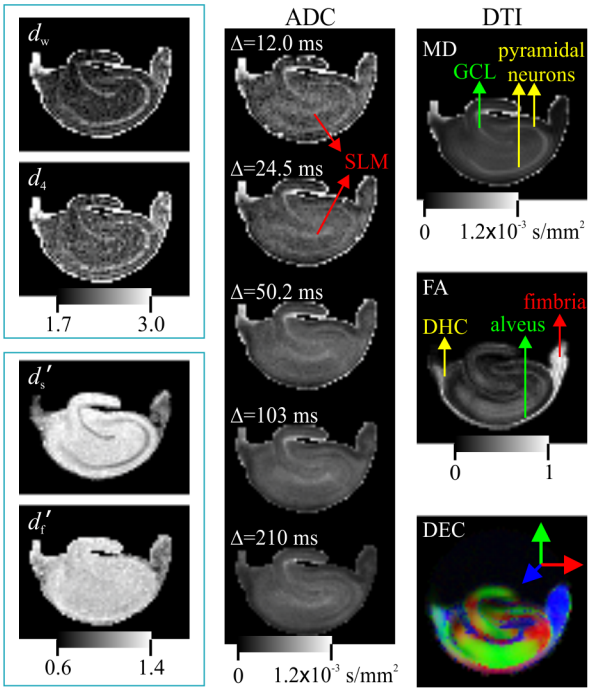

Figure1: Left: Images of the exponents characterizing the TS of the diffusion process. In analogy with d_w, the estimation of d_4 employed the TS of the fourth order moment $\langle z^4\rangle$. Middle: The apparent diffusion coefficient (ADC) maps for all five diffusion times computed from the low-q regime of the data sets. Right: Traditional DTI-derived mean diffusivity (MD), fractional anisotropy (FA), and direction encoded color (DEC) maps computed for the same slice. DHC: dorsal hippocampal commissure, GCL: granule cell layer, SLM: stratum lacunosum-moleculare.

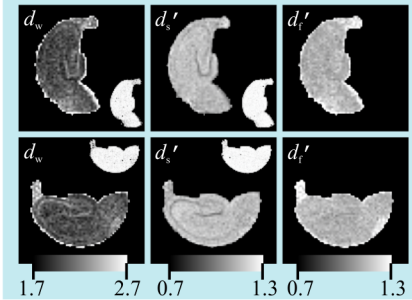

Figure 2: TS parameters are shown for two different excised rat hippocampi scanned at 37°C. Different rows correspond to different specimens. The similarity of the images for different samples suggests the reproducibility of the TS parameters under identical experimental conditions. The adequacy of the TS model is evident in the small images, which show the absolute value of the linear correlation coefficient scaled between 0.9 (black) and 1.0 (white).

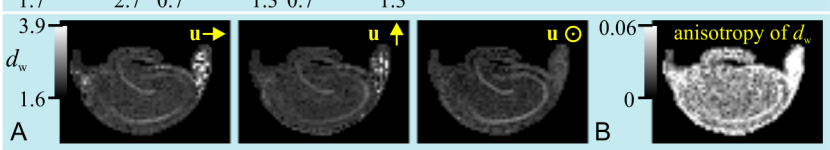

Figure3: A. The three images show the d_w-valued maps computed from the scaling of mean-squared-displacement (MSD) values along the right-left, up-down, and through the slice directions, respectively. B. The image shows the variance of the d_w values computed from the MSD values along 130 directions as a measure of anisotropy in the d_w estimates.